NACA RM L56H21

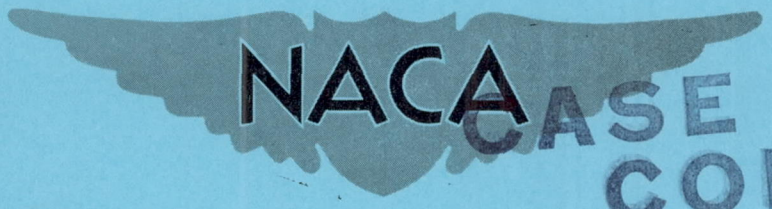

RESEARCH MEMORANDUM

EFFECT OF INCREASE IN ANGLE OF DEAD RISE ON THE HYDRODYNAMIC QUALITIES OF A SEAPLANE CONFIGURATION INCORPORATING HIGH WING LOADING

By Walter J. Kapryan and Irving Weinstein

Langley Aeronautical Laboratory
Langley Field, Va.

NATIONAL ADVISORY COMMITTEE
FOR AERONAUTICS
WASHINGTON

October 31, 1956
Declassified September 17, 1958

NATIONAL ADVISORY COMMITTEE FOR AERONAUTICS

RESEARCH MEMORANDUM

EFFECT OF INCREASE IN ANGLE OF DEAD RISE ON THE HYDRODYNAMIC QUALITIES OF A SEAPLANE CONFIGURATION INCORPORATING HIGH WING LOADING

By Walter J. Kapryan and Irving Weinstein

SUMMARY

An investigation has been made to determine the effects of increase in angle of dead rise on the overall hydrodynamic characteristics of a seaplane having a length-beam ratio of 15 and a wing loading of 120 pounds per square foot.

In general, increasing the angle of dead rise from 20° to 40° and 60° improved the trim limits of stability and the range of center-of-gravity positions for satisfactory take-off characteristics. The 60° hull was characterized by somewhat erratic behavior due to a low trim directional instability. The smooth-water landing characteristics of the 20° and 40° hulls were satisfactory. The 60° hull, however, had somewhat inferior characteristics as evidenced by fairly severe porpoising and skipping. Spray characteristics were, in general, somewhat improved with increase in angle of dead rise. Water resistance, on the other hand, was increased appreciably by the increase in dead-rise angle. Rough-water-landing behavior was definitely improved by the introduction of the higher dead-rise angles. The maximum vertical and angular accelerations of the 20° hull were reduced 42 percent and 35 percent, respectively, by the 40° hull and 72 and 65 percent, respectively, by the 60° hull. The reductions in vertical accelerations are shown to be in good agreement with those predicted by impact theory.

INTRODUCTION

The trend toward higher take-off and landing speeds for current and proposed aircraft has confronted the seaplane designer with the problem of increasingly severe loads and motions in rough water. A recent model investigation in Langley tank no. 1 has shown that

increasing the wing loading of a conventional seaplane from 40 pounds per square foot to 120 pounds per square foot resulted in an increase of approximately 100 percent in the vertical accelerations encountered during landings in waves 4 feet high. These results have led to a number of load-alleviation studies.

One obvious method of reducing the impact effects to which a seaplane hull is subjected is to increase the angle of dead rise of the hull. The effect of an increase in basic dead-rise angle from 20° to 40° was previously investigated with a dynamic model of a seaplane having a wing loading of 40 pounds per square foot. (See ref. 1.) The results of that investigation indicated that the increase in angle of dead rise, in addition to substantially reducing the impact accelerations and motions, maintained acceptable hydrodynamic characteristics in other respects, at least for the relatively low wing loading of 40 pounds per square foot.

The primary purpose of the present paper is to present the results of an investigation into the overall hydrodynamic characteristics of a series of three related dynamic models having basic angles of dead rise of 20°, 40°, and 60° and the relatively high wing loading of 120 pounds per square foot. The models were assumed to be 1/12-scale powered dynamic models of a twin-engine, propeller-driven seaplane having a gross weight of 75,000 pounds, a gross load coefficient of 5.88, and a thrust of 38,800 pounds. The corresponding average landing speed in this case was 120 knots. The configuration with a 20° angle of dead rise was the parent hull for the series and was the same model that was used in the wing loading investigation previously referred to. Power-on smooth-water spray, longitudinal stability, and resistance during take-off, and power-off landing characteristics in smooth water and in waves 4 feet high were determined for all models.

SYMBOLS

b	maximum beam of hull, ft
C_{Δ_o}	gross-load coefficient $\left(\Delta_o/wb^3\right)$
$\bar{c}$	mean aerodynamic chord
g	acceleration due to gravity, ft/sec^2
n_v	vertical acceleration, g units
V	horizontal velocity of model, knots

V_v sinking speed, ft/min

w specific weight of tank water, 63.4 lb/cu ft

α angular acceleration, radians/sec^2

β dead-rise angle, deg

γ flight-path angle, deg

Δ_o gross load, lb

δ_e elevator deflection, deg

τ trim (angle between forebody keel at step and horizontal), deg

τ_L landing trim (trim at contact), deg

DESCRIPTION OF MODELS

The models used for this investigation had basic angles of dead rise of 20°, 40°, and 60° (designated as Langley tank models 318-A, 318-B, and 318-C, respectively) excluding chine flare. Photographs of the models (without propellers) are shown in figure 1. The hull lines are shown in figure 2. The general arrangement for the seaplane with the 20° hull is shown in figure 3. The offsets for the hulls are presented in tables I, II, and III. The 40° and 60° hulls were derived from the basic hull having an angle of dead rise of 20° by maintaining the constant angles of dead rise of 40° and 60° from the step (station 12) forward to station 7. From station 7 forward to the forward perpendicular, the angle of dead rise was uniformly increased so that at the forward perpendicular it was the same as that of the basic 20° hull. At each forebody station the ratio of the flared chine height above the base line to that of the unflared chine height was the same as that of the basic 20° forebody. The respective afterbodies had dead-rise angles of 40° and 60° with no chine flare. All three models had a step depth normal to the base line of 9 percent of the beam.

APPARATUS AND PROCEDURES

A general description of tank no. 1 and the apparatus used is given in references 2 and 3. Each model was free to trim about its pivot,

which was located at the center of gravity, and was free to move vertically but was restrained laterally and in roll and yaw. For the tests in waves, the model had approximately 5 feet of fore-and-aft freedom with respect to the towing carriage. The longitudinal forces on the model which were measured during the determination of excess thrust were obtained by means of a resistance dynamometer connected to the towing gear.

The vertical accelerations were measured with a strain-gage accelerometer mounted on the towing staff of the model. The angular accelerations were measured with a matched pair of accelerometers of the same type located within the model. In the static condition all accelerometers read zero. The natural frequencies of the strain-gage accelerometers were approximately 356 cycles per second for the vertical accelerometers and 180 cycles per second for the angular accelerometers. The natural frequency of the recording galvanometers was approximately 100 cycles per second. The accelerometers were damped to approximately 0.7 of their critical values and the recording galvanometers to approximately 0.65 of their critical values. Additional damping was introduced to make the frequency response curves of the strain-gage-accelerometer and recording-galvanometer systems flat to within ±5 percent between 0 and 27 cycles per second, in accordance with previous tests.

The trim, rise, and fore-and-aft position of the model were measured with slide-wire pickups. During landing approach, the trim of the model in the air was fixed by an electrically actuated trim brake attached to the towing staff. The brake was automatically released when the hull came in contact with the water. Electrical contacts were located at the sternpost, step, and at a point approximately 40 percent of the forebody length aft of the forward perpendicular in order to release the brake and to indicate when these parts of the model contacted or left the water.

The trim and center-of-gravity limits of stability, smooth-water landings, and excess thrust were determined at a gross load corresponding to 83,000 pounds. This represents a design overload slightly in excess of 10 percent. The overload was caused by the heavier weight of the 40° and 60° hulls which, together with the electric motors that powered the models, did not permit balancing the models to the design gross weight of 75,000 pounds. The spray characteristics were determined at gross loads ranging from approximately 46,000 pounds to 100,000 pounds. This range of loads was obtained by means of counterweights.

The trim and center-of-gravity limits of stability and the spray characteristics were determined at the design thrust of 38,800 pounds. The measurements of excess thrust (thrust available for acceleration)

were made with the static thrust set at 45,500 pounds. This increase in power was required to overcome the high drag of the 60° dead-rise hull. The landings in both smooth water and in waves were made with power off.

For the landings in waves, the motors were removed and the tests were made at a gross load of 75,000 pounds. The landing and spray tests were made with the center of gravity at 36 percent mean aerodynamic chord. With the exception of the tables of offsets, all data are presented as full-scale values.

RESULTS AND DISCUSSION

Trim limits of stability.- The trim limits of stability for the three dead-rise models are shown in figure 4. (The trim limit of stability is defined as the trim at which porpoising motion is first observed at a given speed. The general procedure for determining trim limits is described in detail in reference 4.) The increase in angle of dead rise shifted the hump of the lower limit to higher speeds and decreased the hump trim. The hump trim of the 20° hull was approximately 8.5°, while the 40° and 60° hulls had hump trims of approximately 7.2° and 4.9°, respectively. In the planing range the lower limit of the 40° hull was roughly comparable with that of the 20° hull. The upper limit, however, was encountered at slightly higher trims than was that of the 20° hull. Thus, the major changes induced by increasing the angle of dead rise from 20° to 40° appeared to be a decrease in hump trim and a slight shift of the upper limit to higher trims. These findings in general concur with those of reference 1. For the 60° hull the major change in the trim limits, in addition to a significant decrease in hump trim, appeared to be a marked shift of both limits to substantially higher speeds.

The lower trim limit of stability of the 60° hull was difficult to define because of a directional instability which appeared at trims below 5°. At these low trims the model had a strong yawing tendency which was controlled by periodically realining the model and restricting the yaw to small angles by the use of a yoke.

Center-of-gravity limits of stability.- Typical trim tracks for the three hulls covering a range of elevator deflections are presented in figure 5 for a center-of-gravity position of 28 percent mean aerodynamic chord. From such data, maximum amplitudes of porpoising during take-off were determined for a range of center-of-gravity positions. The resulting faired curves defining these amplitudes for the hulls having angles of dead rise of 20° and 40° are presented in figure 6. The center-of-gravity limit of stability for a given elevator deflection

is generally defined as the position of the center of gravity at which the amplitude of porpoising becomes 2°. From this definition and the curves of figure 6, the center-of-gravity limits of stability were determined for the 20° and 40° hulls and are presented as figure 7. As expected from previous tests (ref. 1), the increase in angle of dead rise from 20° to 40° substantially increased the range of elevator settings for acceptable take-offs throughout most of the range of center-of-gravity positions.

The take-off behavior of the 60° hull was noticeably different from that of the other two hulls, and the definition of both the forward and aft limits was more difficult. For moderate increases in bow-up aerodynamic pitching moments (up elevators) the amplitude of upper-limit porpoising increased, as would be expected on the basis of tests of other models. With further increase in up elevator, however, this amplitude of porpoising again decreased, finally becoming negligible. This effect is shown in figure 8, which presents the variation of the maximum amplitude of upper-limit porpoising with elevator deflection at various center-of-gravity positions. The upper limit, it will be recalled, was displaced to significantly higher speeds when the angle of dead rise was increased from 40° to 60°. The decrease in amplitude of upper-limit porpoising with increase in elevator deflection, as shown in figure 8, is believed to be due to the previously mentioned shift of the upper limit to higher speeds which, together with the relatively high trims resulting from the increased elevator deflections, practically made the model airborne when the upper trim limit was reached. As a result, after a mild oscillation or two the model became fully airborne.

The aft limit resulting from the above variation of upper-limit porpoising therefore was defined as a band of instability above and below which the model was stable. (See fig. 9.) For any practical consideration, however, this band of instability is of small consequence since the maximum amplitude of porpoising exceeded 3° at only one center-of-gravity position, and then by less than 0.5°, so that if, as has been done on occasion in the past, a maximum amplitude of porpoising of 3° is considered acceptable for satisfactory take-off performance, the aft limit is of no practical significance.

The definition of a forward limit for the 60° hull was precluded by the previously mentioned directional instability that was encountered at trims below 5°. In its stead, a limit was selected which was defined by the minimum elevator deflections, resulting in trims that did not fall below 5° during any part of the take-off run (fig. 9). Since the lower trim limit of stability is in its entirety encountered at trims lower than 5°, such a procedure will insure take-offs with acceptable longitudinal stability and without directional instability.

Landing stability.- Typical time histories of landings with the three hulls are presented in figure 10. From records such as these, the maximum and minimum values of trim and rise at the greatest cycle of oscillation were determined and the resulting data are plotted against trim at first contact in figure 11. The 20° and 40° hulls exhibited practically no skipping tendencies over the range of landing trim from 4.5° to 15°. The 60° hull, however, skipped at all trims below 8.5° and above 12.3° and its porpoising cycles were greater than those of the other models at all trims.

The inferior landing characteristics of the 60° hull are probably due to a combination of inadequate step ventilation (the ratio of step depth to maximum beam being only 0.09) and the deep penetration of the afterbody resulting from the high angle of dead rise. The resultant wetting of the sides of the afterbody with the clinging flow of the forebody wake appears to have produced suction forces that maintained trims high enough to keep the model in the range of upper-limit instability longer than was the case for the models of lower dead-rise angle. This situation probably could have been somewhat relieved by increasing the step depth. Also, for these smooth-water landings, all three models were decelerated at the same rate. A more realistic procedure probably would have been to decelerate the 60° hull at a greater rate to simulate the deceleration that would occur in free flight due to the high resistance of this hull. The resulting porpoising cycles would undoubtedly have been less violent. Thus, although the 60° hull has inferior smooth-water landing characteristics when compared with the 20° and 40° hulls, a more favorable comparison might have been obtained if the need for a deeper step had been anticipated and a higher deceleration, corresponding to a higher resistance, had been used.

Spray characteristics.- The spray characteristics of the three hulls are presented in figure 12, where the range of speed over which spray entered the propellers or struck the flaps and tail surfaces is plotted against gross load. In general, the spray entering the propellers and striking the flaps has been somewhat alleviated by increasing the angle of dead rise. (Although the 40° configuration did encounter heavy spray at lighter gross loads than did the 20° model, the speed range over which this spray was encountered was almost negligibly small and was not considered serious. In any case, for the 20° model the overall propeller and flap spray diagrams, which include light as well as heavy spray, extended over a significantly greater speed range than for the other two models at practically all gross loads.) The smaller bow blister resulting from the increased dead-rise angle is believed to be the chief factor in this general reduction. These results are in keeping with the results of previous investigations into the effects of increase in angle of dead rise. Tail spray, however, does not appear to have been greatly affected by increasing the dead-rise angle.

Excess thrust.- A brief investigation of the excess thrust was made in order to obtain some measure of the relative resistances of the three hulls. Because of the anticipated high resistance of the 60° hull, which would have precluded its take-off at full thrust, the static thrust for these measurements was arbitrarily increased to 45,500 pounds. The resulting excess thrust and associated trim curves for the three hulls are presented in figure 13. Increasing the angle of dead rise substantially reduced the excess thrust available for take-off, with the increase from 20° to 40° and 60° resulting in reductions of approximately 40 percent and 55 percent, respectively. For the investigation reported in reference 1, an increase in angle of dead rise from 20° to 40° at a wing loading of 40 pounds per square foot resulted in a reduction in available thrust of approximately 30 percent, so that this condition has been somewhat worsened by increasing the wing loading to 120 pounds per square foot and having a depth of step of 9 percent of the beam.

Landings in waves.- The data obtained during landings in waves are presented as full-scale values in tables IV, V, and VI. These tables contain the pertinent information regarding the impacts producing the maximum vertical and angular accelerations encountered with the hulls having angles of dead rise of 20°, 40°, and 60°, respectively. The maximum vertical and angular accelerations are plotted in figure 14.

The maximum accelerations generally occurred at some impact subsequent to the initial impact. For the 20° hull, they generally occurred during the third or fourth impact; for the 40° hull, they generally occurred during the fourth or fifth impact; and, for the 60° hull, they generally occurred during the fourth impact. The vertical accelerations were significantly reduced by the increases in angle of dead rise. The 20° hull experienced maximums as high as 13.4g, while the maximum encountered with the 40° hull was 7.8g, a reduction of approximately 42 percent. This reduction is slightly less than that obtained for the same increase in angle of dead rise at the relatively low wing loading of 40 pounds per square foot as reported in reference 1. The 60° hull experienced a maximum vertical acceleration of 3.7g, which, when compared with the 20° hull, represents a reduction of approximately 72 percent. Corresponding reductions in the angular accelerations resulted from the increase in angle of dead rise. The 40° hull reduced the maximum angular accelerations approximately 35 percent below those of the 20° hull, while the 60° hull produced reductions of approximately 65 percent.

The results of a brief comparison with impact theory (as discussed in ref. 5) of the effect of increase in dead-rise angle on the vertical accelerations are shown in figure 15. Reference 5 states that the hydrodynamic load varies as the 2/3 power of the dead-rise function

$f(\beta) = \frac{\pi}{2\beta} - 1$, other parameters being held the same. By normalizing the curve of the dead-rise function to $\beta = 20^\circ$, the effect of increasing the angle of dead rise during the present investigation can be seen to be in good agreement with theory. The theory, of course, was derived for somewhat different conditions than were encountered during the present investigation and, although it does not predict the same load factors, it is nevertheless interesting to note the excellent agreement in trend.

The maximum and minimum values of the trim and rise at the greatest cycle of oscillation during each of these landings in waves have been plotted against wavelength and are presented in figure 16. Increasing the angle of dead rise resulted in slightly lower trim cycles. The rise cycles were also reduced, only slightly with the 40° hull, but very substantially with the 60° hull.

CONCLUDING REMARKS

The results of an investigation to determine the effect of increase in angle of dead rise on the hydrodynamic qualities of a seaplane having a wing loading of 120 pounds per square foot indicate that very significant reductions in impact loads can be achieved by increasing the angle of dead rise from 20° to 40° and 60°. The 40° hull reduced the maximum vertical accelerations of the 20° hull by approximately 42 percent, while use of the 60° hull resulted in reductions of the order of 72 percent. These reductions are shown to be consistent with theory. The 40° and 60° hulls, in general, improved the trim and center-of-gravity limits of stability as characterized by milder porpoising behavior during takeoff. However, the behavior of the 60° hull was somewhat erratic because of a low trim directional instability. The 40° hull had satisfactory smooth-water-landing characteristics which were comparable with those of the 20° hull. The 60° hull, however, was somewhat inferior to the other two hulls in this respect, inasmuch as fairly large porpoising amplitudes and skipping were encountered with this hull. The spray characteristics were, in general, improved by increasing the angle of dead rise. The

water resistance as measured during a brief evaluation of excess thrust was significantly increased by the respective increases in angle of dead rise.

Langley Aeronautical Laboratory,
National Advisory Committee for Aeronautics,
Langley Field, Va., August 15, 1956.

REFERENCES

1. Whitaker, Walter E., Jr., and Bryce, Paul W., Jr.: Effect of an Increase in Angle of Dead Rise on the Hydrodynamic Characteristics of a High-Length-Beam-Ratio Hull. NACA TN 2297, 1951.

2. Truscott, Starr: The Enlarged N.A.C.A. Tank, and Some of Its Work. NACA TM 918, 1939.

3. Parkinson, John B.: NACA Model Investigations of Seaplanes in Waves. NACA TN 3419, 1955.

4. Olson, Roland E., and Land, Norman S.: Methods Used in the NACA Tank for the Investigation of the Longitudinal-Stability Characteristics of Models of Flying Boats. NACA Rep. 753, 1943. (Supersedes NACA WR L-409.)

5. Edge, Philip M., Jr.: Hydrodynamic Impact Loads in Smooth Water for a Prismatic Float Having an Angle of Dead Rise of 40°. NACA TN 1775, 1949.

TABLE I.- OFFSETS FOR LANGLEY TANK MODEL 318-A

[$\beta = 20°$; all dimensions are in inches]

FOREBODY														AFTERBODY				
Station	Distance to forward perpendicular	Keel above base line	Chine above base line	Half-beam at chine	Angle of chine flare, deg	Forebody bottom, height above base-line buttocks								Station	Distance to forward perpendicular	Keel above base line	Half-beam at chine	Dead-rise angle, deg
						0.30	0.59	0.89	1.18	1.48	1.77	2.07	2.37	2.67					
F.P.	0	8.58	8.58	0	--	----	----	----	----	----	----	----	----	----	12A	50.42	0.52	2.92	20
1/2	2.10	4.57	6.24	1.37	10	5.16	5.76	6.15	6.25	----	----	----	----	----	13	54.58	.92	2.87	20
1	4.20	3.13	4.88	1.82	10	3.58	4.05	4.52	4.79	4.92	4.89	----	----	----	14	58.78	1.32	2.76	20
2	8.40	1.52	3.16	2.29	10	1.87	2.19	2.53	2.82	3.04	3.17	3.20	----	----	15	62.98	1.71	2.58	20
3	12.60	.67	2.12	2.56	10	.91	1.17	1.42	1.67	1.89	2.04	2.12	2.14	----	16	67.17	2.11	2.37	20
4	16.79	.22	1.47	2.73	10	.42	.61	.81	1.00	1.18	1.33	1.45	1.50	1.47	17	71.37	2.51	2.07	20
5	20.99	.03	1.08	2.84	10	.18	.33	.48	.63	.78	.91	1.02	1.09	1.11	18	75.57	2.90	1.70	20
6	25.19	0	.89	2.90	5	.12	.23	.35	.47	.58	.70	.79	.87	.90	19	79.77	3.30	1.22	20
7	29.39	0	.83	2.92	0	.11	.22	.34	.43	.54	.65	.73	.79	.83	20	83.97	3.70	.62	20
8	33.59	0	.83	2.92	0	.11	.22	.34	.43	.54	.65	.73	.79	.83	S.P.	87.61	4.04	0	--
9	37.78	0	.83	2.92	0	.11	.22	.34	.43	.54	.65	.73	.79	.83					
10	41.98	0	.83	2.92	0	.11	.22	.34	.43	.54	.65	.73	.79	.83					
11	46.18	0	.83	2.92	0	.11	.22	.34	.43	.54	.65	.73	.79	.83					
12F	50.42	0	.83	2.92	0	.11	.22	.34	.43	.54	.65	.73	.79	.83					

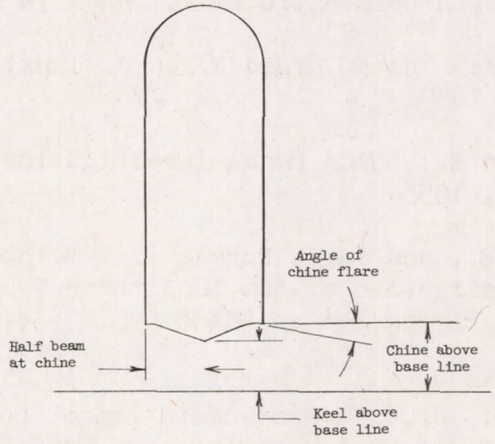

TABLE II.- OFFSETS FOR LANGLEY TANK MODEL 318-B

[β = 40°; all dimensions are in inches]

FOREBODY														AFTERBODY				
Station	Distance to forward perpendicular	Keel above base line	Chine above base line	Half-beam at chine	Angle of chine flare, deg	Forebody bottom, height above base-line buttocks								Station	Distance to forward perpendicular	Keel above base line	Half-beam at chine	Dead-rise angle, deg
						0.30	0.59	0.89	1.18	1.48	1.77	2.07	2.37	2.67					
F.P.	0	8.58	8.58	0	--	----	----	----	----	----	----	----	----	----	12A	50.42	0.52	2.92	40
1/2	2.10	4.57	6.74	1.37	10	5.30	6.01	6.54	6.75	----	----	----	----	----	13	54.58	.92	2.87	40
1	4.20	3.13	5.62	1.82	10	3.74	4.36	4.97	5.43	5.61	5.63	----	----	----	14	58.78	1.32	2.76	40
2	8.40	1.52	4.21	2.29	10	2.04	2.56	3.06	3.57	4.01	4.17	4.22	----	----	15	62.98	1.71	2.58	40
3	12.60	.67	3.30	2.56	10	1.09	1.54	1.97	2.40	2.83	3.15	3.29	3.32	----	16	67.17	2.11	2.37	40
4	16.79	.22	2.70	2.73	10	.61	.98	1.36	1.74	2.12	2.43	2.63	2.72	2.71	17	71.37	2.55	2.07	40
5	20.99	.03	2.32	2.84	10	.36	.68	1.00	1.33	1.66	1.97	2.19	2.31	2.35	18	75.57	2.90	1.70	40
6	25.19	0	2.05	2.90	5	.27	.53	.81	1.07	1.35	1.62	1.85	1.99	2.06	19	79.77	3.30	1.22	40
7	29.39	0	1.92	2.92	0	.25	.50	.74	.99	1.24	1.47	1.67	1.82	1.90	20	83.97	3.70	.62	40
8	33.59	0	1.92	2.92	0	.25	.50	.74	.99	1.24	1.47	1.67	1.82	1.90	S.P.	87.61	4.04	0	--
9	37.78	0	1.92	2.92	0	.25	.50	.74	.99	1.24	1.47	1.67	1.82	1.90					
10	41.98	0	1.92	2.92	0	.25	.50	.74	.99	1.24	1.47	1.67	1.82	1.90					
11	46.18	0	1.92	2.92	0	.25	.50	.74	.99	1.24	1.47	1.67	1.82	1.90					
12F	50.42	0	1.92	2.92	0	.25	.50	.74	.99	1.24	1.47	1.67	1.82	1.90					

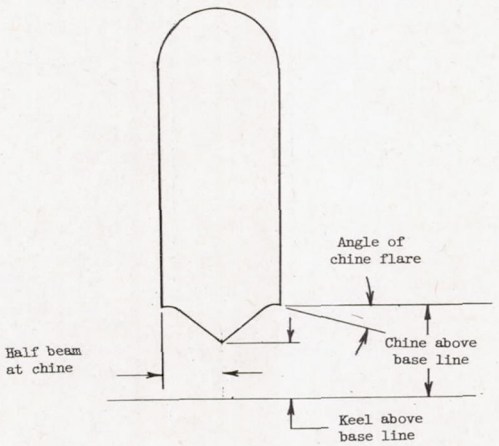

TABLE III.- OFFSETS FOR LANGLEY TANK MODEL 318-C

[β = 60°; all dimensions are in inches]

FOREBODY															AFTERBODY				
Station	Distance to forward perpendicular	Keel above base line	Chine above base line	Half-beam at chine	Angle of chine flare, deg	Forebody bottom, height above base-line buttocks									Station	Distance to forward perpendicular	Keel above base line	Half-beam at chine	Dead-rise angle, deg
						0.30	0.59	0.89	1.18	1.48	1.77	2.07	2.37	2.67					
F.P.	0	8.58	8.58	0	--	----	----	----	----	----	----	----	----	----	12A	50.42	0.52	2.92	60
1/2	2.10	4.57	7.06	1.37	10	5.29	5.99	6.66	6.99	----	----	----	----	----	13	54.58	.92	2.87	60
1	4.20	3.13	5.98	1.82	10	3.83	4.51	5.18	5.66	5.92	6.00	----	----	----	14	58.78	1.32	2.76	60
2	8.40	1.52	4.93	2.29	10	2.18	2.83	3.49	4.09	4.55	4.78	4.90	----	----	15	62.98	1.71	2.58	60
3	12.60	.67	4.44	2.56	10	1.30	1.94	2.57	3.16	3.72	4.09	4.34	4.45	----	16	67.17	2.11	2.37	60
4	16.79	.22	4.17	2.73	10	.82	1.40	2.00	2.58	3.15	3.62	3.95	4.12	4.16	17	71.37	2.55	2.07	60
5	20.99	.03	4.00	2.84	10	.60	1.15	1.73	2.28	2.80	3.31	3.66	3.88	3.99	18	75.57	2.90	1.70	60
6	25.19	0	3.96	2.90	5	.53	1.04	1.57	2.08	2.60	3.11	3.51	3.78	3.94	19	79.77	3.30	1.22	60
7	29.39	0	3.96	2.92	0	.53	1.02	1.54	2.05	2.57	3.04	3.48	3.75	3.92	20	83.97	3.70	.62	60
8	33.59	0	3.96	2.92	0	.53	1.02	1.54	2.05	2.57	3.04	3.48	3.75	3.92	S.P.	87.61	4.04	0	--
9	37.78	0	3.96	2.92	0	.53	1.02	1.54	2.05	2.57	3.04	3.48	3.75	3.92					
10	41.98	0	3.96	2.92	0	.53	1.02	1.54	2.05	2.57	3.04	3.48	3.75	3.92					
11	46.18	0	3.96	2.92	0	.53	1.02	1.54	2.05	2.57	3.04	3.48	3.75	3.92					
12F	50.42	0	3.96	2.92	0	.53	1.02	1.54	2.05	2.57	3.04	3.48	3.75	3.92					

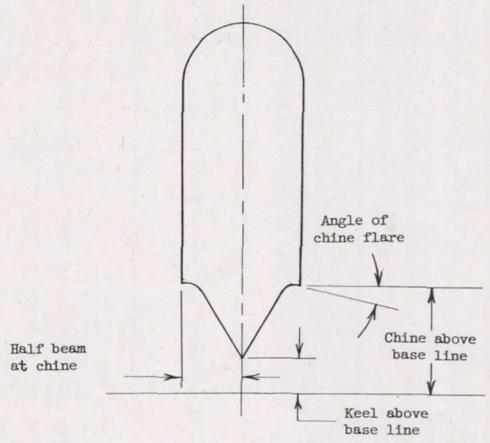

TABLE IV

DATA OBTAINED DURING LANDINGS IN 4-FOOT WAVES

[$\beta = 20^\circ$; all values are full-scale; initial landing trim $\approx 8^\circ$]

Landing	Wavelength, ft	At maximum acceleration					
		τ_L, deg	V_V, ft/min	V, knots	γ, deg	n_V, g units	α, radians/sec^2
1	180	2.3	1037	107.5	5.5	9.8	18.3
2	180	4.6	1410	66.4	11.8	7.8	13.3
*	180	2.4	675	107.2	3.6	7.1	15.7
3	180	1.2	1375	96.0	8.1	10.2	22.3
4	180	1.5	1530	96.4	8.9	10.6	21.5
5	180	1.4	994	97.5	5.8	6.9	16.9
6	180	2.9	1203	103.2	6.6	10.7	19.7
7	180	3.0	1222	105.8	6.5	9.3	17.0
8	180	3.6	1037	77.5	7.5	9.4	18.6
9	180	.9	1353	84.8	9.0	7.2	20.9
10	180	5.3	1196	70.8	9.5	7.5	----
11	180	3.8	391	105.7	2.1	6.6	----
12	180	.8	1825	89.0	11.4	8.3	----
13	180	4.1	1298	71.8	10.1	10.2	----
14	180	1.5	1275	91.1	7.1	9.4	----
15	180	.7	1390	84.8	9.2	9.3	----
16	180	.4	1380	87.9	6.6	8.0	16.7
17	180	2.0	1130	95.0	6.7	8.1	14.2
18	180	1.4	1393	102.6	7.6	9.8	16.0
19	180	.9	1374	87.3	8.7	10.6	19.5
20	180	-.7	1420	78.6	10.1	9.4	17.8
21	180	1.8	1058	106.4	5.6	8.2	13.5
22	180	1.1	1503	92.5	9.1	7.7	18.1
23	180	3.3	555	104.0	3.0	5.3	7.9
24	180	1.2	1257	91.0	7.8	7.7	15.3
25	180	-.1	1303	97.3	7.5	8.3	18.3
26	180	1.3	1420	85.3	9.3	11.4	20.9
27	180	.4	1286	86.5	8.3	8.1	17.6
28	180	.7	1561	80.6	10.8	12.1	23.2
29	216	1.6	1530	77.7	11.0	9.6	19.1
30	216	2.4	1479	106.4	7.8	11.7	22.6
31	216	1.4	1452	93.6	8.7	9.7	19.2
32	216	1.7	1051	85.7	6.9	8.6	17.3
33	216	1.7	1394	74.0	10.5	11.3	20.7
34	216	2.6	1354	104.9	7.3	9.0	23.0
35	216	1.7	1371	72.5	10.6	9.9	21.1
36	216	2.4	1648	103.7	8.9	11.9	23.9
37	216	.8	1662	93.4	10.0	9.9	20.4
38	216	2.8	1378	103.5	7.5	12.6	24.4
39	216	2.3	1388	103.3	7.5	12.6	24.2
40	216	2.0	1137	101.7	6.3	8.9	17.2
41	216	1.2	1230	73.7	9.4	5.6	----
42	216	1.0	1271	76.7	9.3	10.0	----

TABLE IV.- Concluded

DATA OBTAINED DURING LANDINGS IN 4-FOOT WAVES

[β = 20°; all values are full-scale; initial landing trim ≈ 8°]

Landing	Wavelength, ft	At maximum acceleration					
		τ_L, deg	V_V, ft/min	V, knots	γ, deg	n_V, g units	α, radians/sec^2
43	216	2.6	956	84.4	6.4	10.2	----
44	216	2.3	652	95.2	3.9	7.5	----
45	216	1.7	1108	101.9	6.1	9.7	18.1
46	216	1.9	935	103.8	5.1	9.0	15.8
47	216	2.6	952	72.6	7.4	7.5	14.8
48	216	3.9	914	86.7	5.9	6.4	8.1
49	216	.3	567	94.1	3.4	5.8	8.3
50	216	-.6	1448	92.3	8.8	7.4	18.4
51	216	-1.9	1488	79.1	10.5	10.2	17.3
52	216	2.3	787	106.7	4.2	7.5	11.9
53	216	5.0	1027	78.1	7.4	7.0	10.1
54	216	4.9	498	106.9	2.9	4.1	5.8
55	216	-.7	1430	96.2	8.4	7.1	17.7
56	216	1.8	1321	77.9	9.5	9.2	13.7
57	252	1.3	1393	103.0	7.6	7.6	13.6
58	252	1.9	1576	92.3	9.6	9.7	19.7
59	252	1.7	1348	81.9	9.2	10.3	20.7
60	252	1.5	1371	88.0	8.8	9.6	17.3
61	252	1.6	1257	99.4	7.1	10.7	21.6
62	252	2.9	775	101.9	4.3	6.2	12.4
63	252	1.1	1260	89.2	7.9	9.1	17.3
64	252	.8	1468	74.3	11.0	8.8	17.7
65	252	1.0	1547	95.7	9.0	10.2	20.7
66	252	1.3	1178	85.3	7.8	8.8	17.3
67	252	.9	1253	98.7	7.1	10.3	22.0
68	252	1.3	1243	86.2	8.2	9.9	----
69	252	0	1579	80.3	11.0	10.2	----
70	252	2.1	1147	89.1	7.2	8.4	----
71	252	1.7	1410	95.1	8.3	13.4	----
72	252	-.1	----	99.4	----	8.1	17.7
73	252	.7	1160	102.5	6.4	8.2	15.9
74	252	1.6	1323	76.7	9.6	11.4	21.8
75	252	2.1	1240	79.6	8.8	11.0	20.2
76	252	.5	1373	97.0	8.0	8.9	15.7
77	252	2.6	978	104.2	5.3	7.8	11.6
78	252	1.7	913	71.0	7.2	7.3	13.0
79	252	2.3	896	103.8	4.9	8.4	14.4
80	252	1.7	891	103.2	4.9	8.1	15.3
81	252	.8	1057	82.7	7.2	8.7	15.3
82	252	2.4	810	110.9	4.1	6.4	9.6
83	252	.9	1271	85.0	8.4	9.5	16.2
84	288	.6	1430	81.5	9.8	10.7	20.0
85	288	1.4	1679	99.1	9.5	11.4	22.8

TABLE V

DATA OBTAINED DURING LANDINGS IN 4-FOOT WAVES

[β = 40°; all values are full-scale; initial landing trim ≈ 8°]

Landing	Wavelength, ft	At maximum acceleration					
		τ_L, deg	V_v, ft/min	V, knots	γ, deg	n_v, g units	α, radians/sec^2
1	180	1.9	1100	93.5	6.6	5.6	11.2
2	180	5.7	976	76.0	7.2	5.0	6.5
*	180	2.7	700	87.2	4.5	3.5	7.7
3	180	5.3	1123	68.3	9.2	3.8	7.7
4	180	4.7	----	89.0	----	4.4	6.5
5	180	3.1	945	76.7	6.9	4.6	8.8
6	180	4.7	1220	69.3	9.8	4.6	7.0
7	180	2.5	1090	93.0	6.6	5.0	7.7
8	180	5.5	1045	72.8	8.1	5.8	8.3
9	180	4.6	852	82.6	5.8	4.7	7.7
10	180	1.6	945	97.3	5.5	4.6	8.7
11	180	3.3	1098	76.2	8.1	5.6	9.9
12	216	5.0	318	116.8	1.5	3.3	4.2
13	216	1.1	1373	91.4	8.4	6.7	13.5
14	216	2.5	1058	81.0	7.3	5.7	9.1
15	216	4.5	780	91.6	4.8	3.7	5.2
16	216	1.5	1268	94.0	7.6	4.8	6.5
17	216	-.1	1805	86.5	11.6	6.5	15.0
18	216	3.5	1008	80.3	7.0	5.1	8.3
19	216	7.3	900	53.5	9.4	3.0	5.2
20	216	.3	1638	86.2	10.6	6.7	13.5
21	216	3.7	995	84.7	6.6	4.9	8.3
22	216	.7	1690	87.0	10.9	7.4	15.6
23	216	8.1	758	65.0	6.6	2.8	----
24	216	5.1	783	92.2	4.8	4.1	----
25	216	.8	1523	90.7	9.4	5.2	----
26	216	2.2	1384	96.8	8.0	5.2	----
27	216	4.3	1056	82.3	7.2	5.7	----
28	216	2.0	1270	97.7	7.3	5.9	----
29	216	2.1	1503	94.3	8.9	7.8	----
30	216	3.3	1343	77.3	9.7	4.6	----
31	216	5.2	1070	77.3	7.8	3.1	----
32	252	6.4	752	64.4	6.6	2.2	3.7
33	252	5.2	792	70.2	6.4	3.1	4.3
34	252	2.7	755	105.8	4.1	2.8	4.8
35	252	1.6	1233	84.7	8.2	5.5	9.5
36	252	1.9	1260	97.7	7.2	7.1	11.7
37	252	4.5	388	117.3	1.9	2.7	3.1
38	252	1.3	1418	91.2	9.0	2.6	3.3
39	252	2.2	898	104.3	4.9	4.2	7.2
40	252	.7	1357	92.3	8.2	6.2	10.8
41	252	1.1	1280	80.0	9.0	5.4	9.8
42	252	5.2	820	69.5	6.6	3.2	4.4
43	288	2.3	1123	93.0	6.8	4.2	6.3
44	288	4.7	484	109.8	2.5	2.6	2.3
45	288	2.7	980	104.3	5.3	4.2	6.7
46	288	2.4	1136	93.0	6.9	5.2	8.3
47	288	2.5	923	96.8	5.4	3.9	6.3
48	288	3.1	1110	104.0	6.2	5.3	7.0
*	288	2.4	1172	92.3	7.2	4.6	7.7
49	288	2.7	853	97.8	4.9	4.5	7.2
50	288	4.1	973	65.6	8.3	3.8	6.2
51	324	1.3	1217	91.0	7.5	5.2	9.4
52	324	1.6	1202	93.6	7.2	4.3	7.5
53	324	2.7	1093	97.3	6.2	3.0	3.6
54	324	2.0	1386	91.5	8.5	6.0	10.1
55	324	6.3	865	65.0	7.5	3.5	4.6
*	324	1.6	942	74.3	7.1	2.9	6.2
56	324	1.7	1140	93.5	6.9	4.9	8.8
57	324	2.6	1160	107.5	6.1	6.5	9.3
58	324	2.3	1174	97.4	6.8	4.4	6.2

TABLE VI

DATA OBTAINED DURING LANDINGS IN 4-FOOT WAVES

[$\beta = 60°$; all values are full-scale; initial landing trim $\approx 8°$]

Landing	Wavelength, ft	At maximum acceleration					
		τ_L, deg	V_v, ft/min	V, knots	γ, deg	n_v, g units	α, radians/sec^2
1	180	3.8	387	118.3	1.9	2.1	3.7
2	180	2.5	992	94.3	5.9	3.7	8.1
3	180	1.2	1285	90.8	7.9	3.2	8.3
4	180	3.8	813	90.7	5.1	2.3	3.6
5	180	4.1	1080	82.0	7.4	3.3	7.2
6	180	5.2	368	119.0	1.8	1.8	2.6
*	180	3.5	476	83.2	3.2	1.3	4.4
7	180	2.5	604	88.8	3.9	2.9	8.7
8	180	3.2	447	81.2	3.1	1.4	3.9
9	180	2.7	569	92.3	3.5	2.3	6.3
10	180	5.0	756	92.6	4.6	3.0	4.4
*	180	1.5	859	95.1	5.1	2.5	6.5
11	180	2.4	993	94.7	5.9	3.5	8.5
12	180	3.0	623	86.7	4.1	2.5	5.7
13	216	3.1	738	104.1	4.0	2.4	4.4
14	216	3.1	758	105.8	4.0	2.4	4.7
15	216	2.5	513	107.6	2.7	2.1	3.9
16	216	1.1	792	107.7	4.2	2.6	5.7
17	216	1.8	523	106.0	2.8	1.7	2.7
18	216	2.5	820	85.5	5.4	2.0	4.3
19	216	4.0	975	81.8	6.7	2.8	5.7
20	216	2.2	765	108.5	4.0	2.7	6.9
21	216	3.9	825	87.5	5.3	3.4	7.4
22	216	3.5	935	80.5	6.5	2.3	5.2
23	216	4.4	478	83.4	3.2	1.6	4.1
24	252	2.3	901	89.5	5.7	2.9	6.2
25	252	2.6	1055	90.8	6.5	3.3	6.8
26	252	3.1	990	89.5	6.2	3.4	6.8
27	252	2.4	985	93.3	6.0	2.8	5.8
28	252	2.4	1010	94.7	6.0	2.5	4.7
29	252	2.4	1170	89.2	7.4	3.1	6.7
30	252	2.8	1040	84.9	6.9	2.0	4.2
31	252	3.0	----	95.0	---	2.2	4.6
32	252	3.5	856	95.0	5.1	2.8	5.4
33	252	2.7	1040	89.7	6.5	3.2	6.4
34	252	2.5	1017	88.7	6.4	2.3	4.7
35	252	4.7	430	92.4	2.6	1.4	2.1
36	288	1.7	1055	96.2	6.2	2.9	5.7
37	288	7.0	293	118.3	1.4	1.7	2.1
38	288	1.2	1215	92.1	7.4	3.0	7.3
39	288	2.3	1010	90.1	6.3	2.5	5.2
40	288	1.4	1104	93.5	6.6	2.9	6.8
41	288	4.5	437	118.8	2.1	2.0	2.6
42	288	3.1	659	86.2	4.3	1.4	3.4
43	288	3.8	474	118.8	2.3	1.8	4.2
44	288	3.6	753	84.4	5.0	1.8	4.4
45	324	3.2	730	105.4	3.9	1.7	2.0
46	324	5.0	672	81.4	4.7	1.8	2.6
47	324	3.5	484	117.8	2.3	1.9	3.4
48	324	4.7	432	120.8	2.0	1.9	2.6
49	324	3.2	442	117.6	2.2	1.9	3.1
50	324	5.6	775	72.5	6.0	2.1	3.4
*	324	2.5	637	85.8	4.2	1.7	4.4
51	324	2.9	852	105.0	4.6	2.3	3.6
52	324	3.4	944	100.5	5.3	2.8	4.1

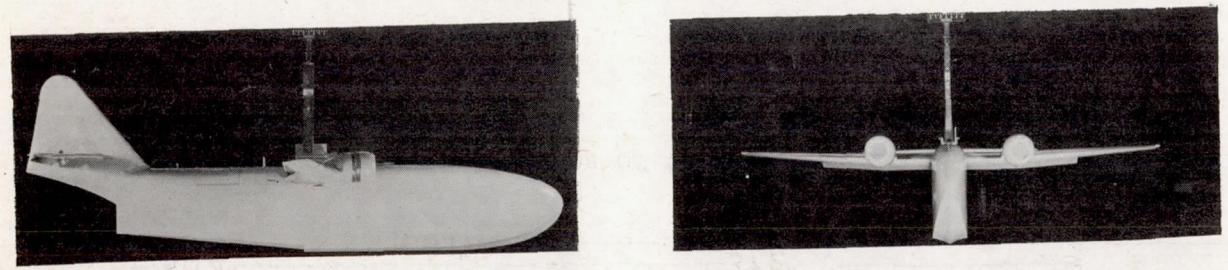

(a) $\beta = 20^{\circ}$.

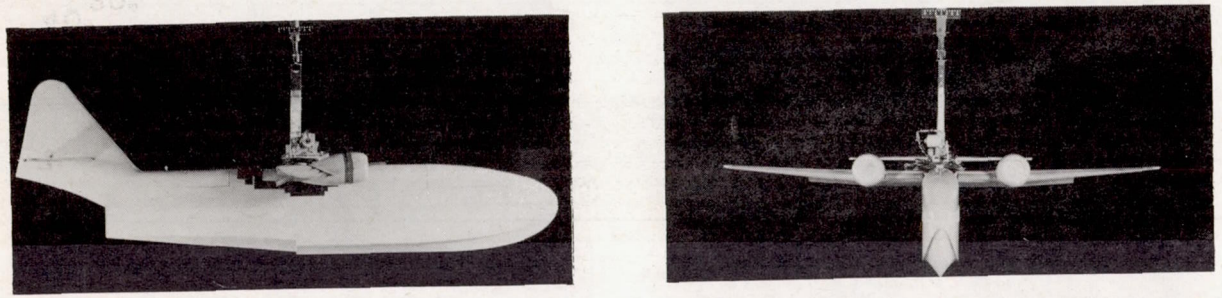

(b) $\beta = 40^{\circ}$.

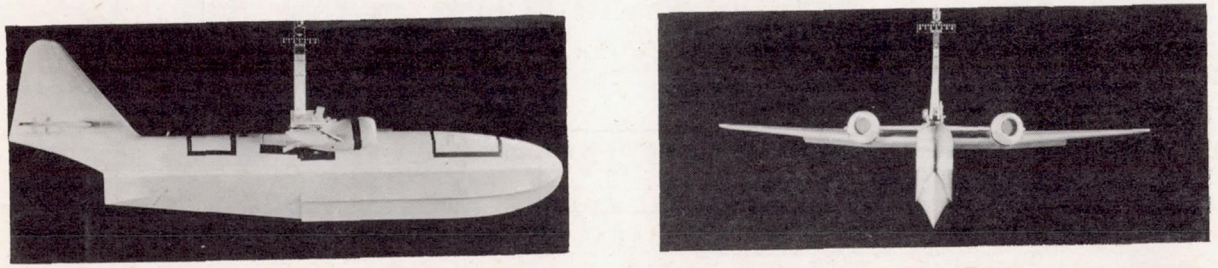

L-95775

(c) $\beta = 60^{\circ}$.

Figure 1.- Photographs of models.

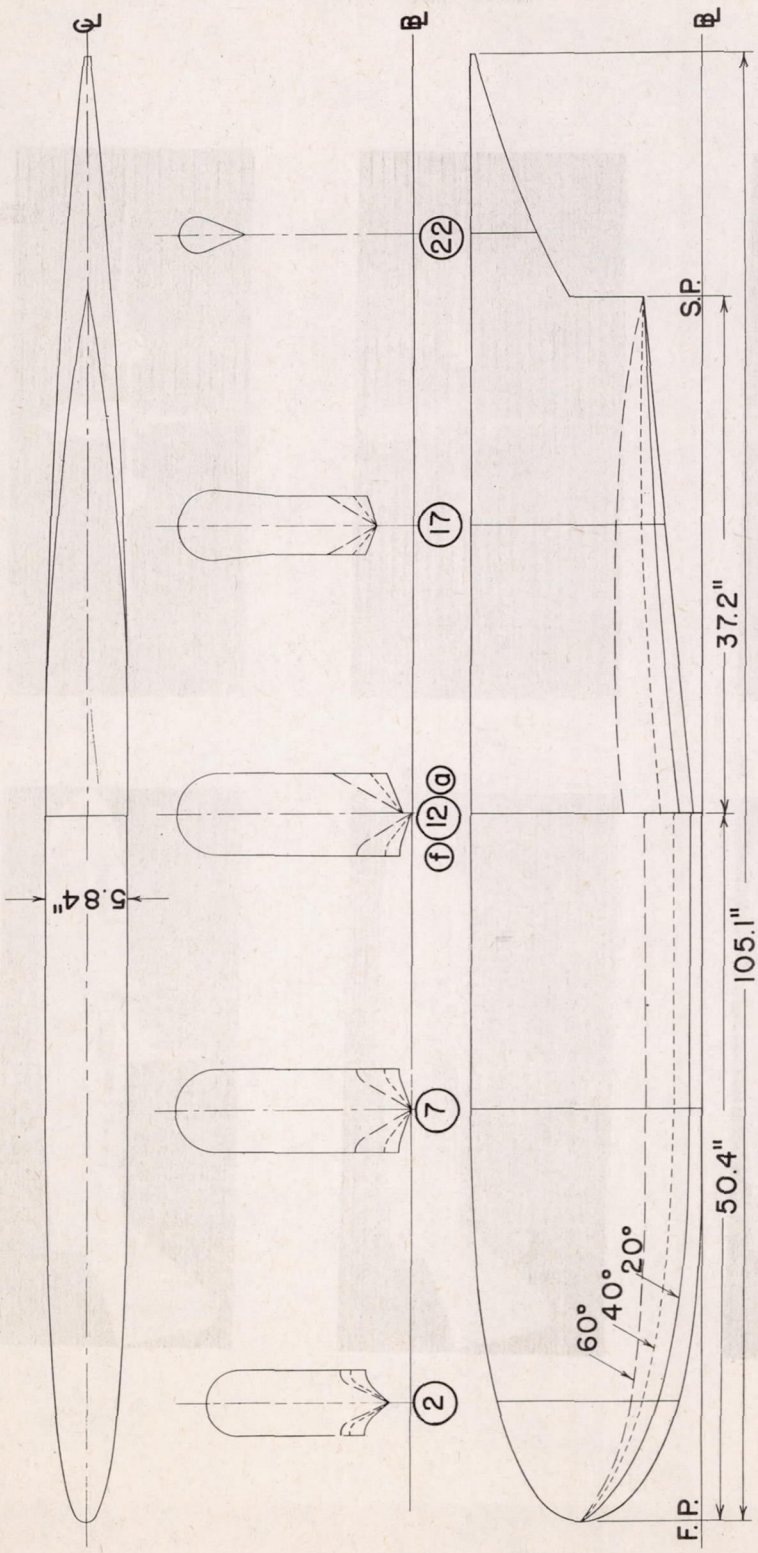

Figure 2.- Hull lines of test models.

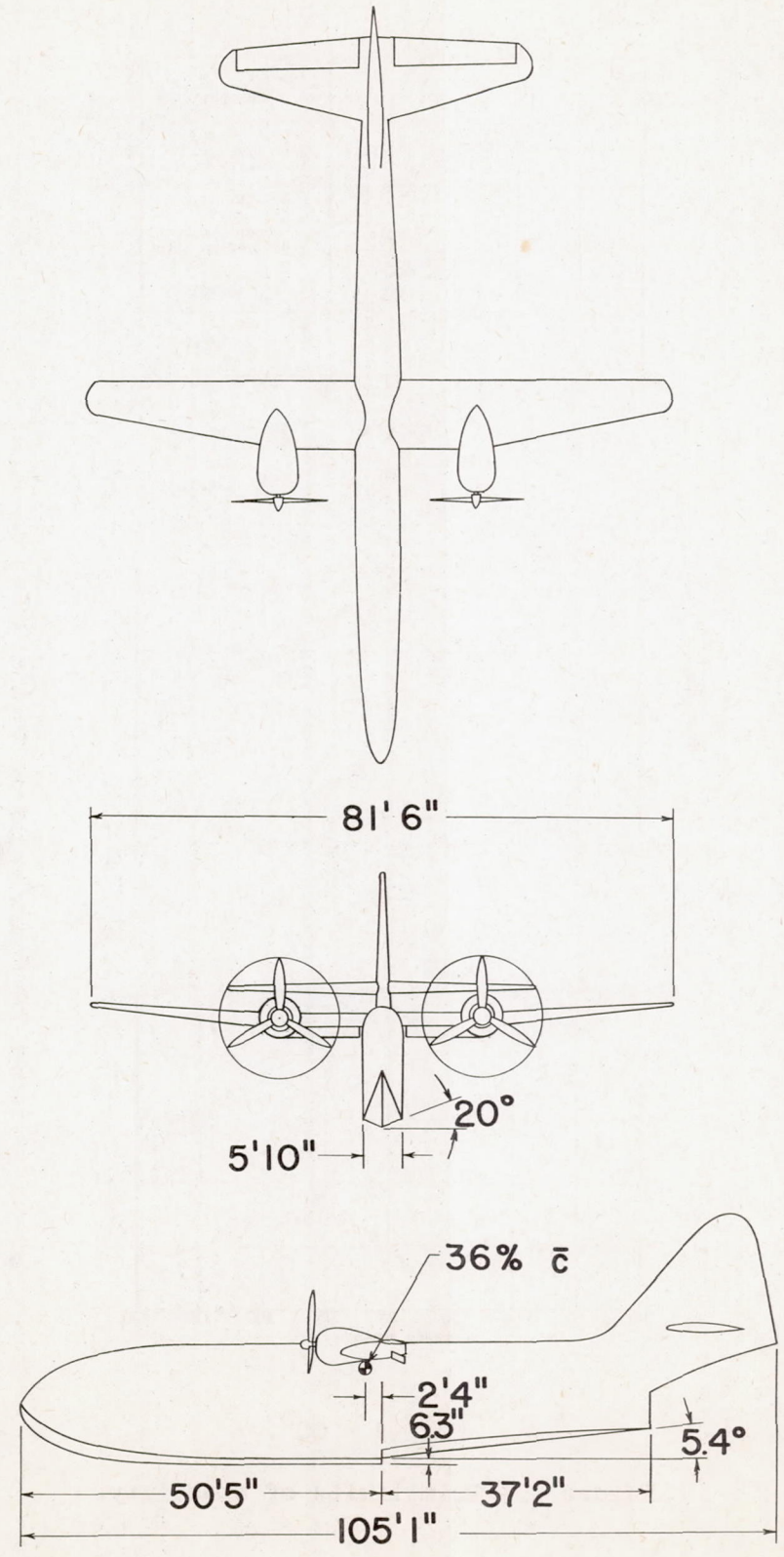

Figure 3.- General arrangement of test configuration.

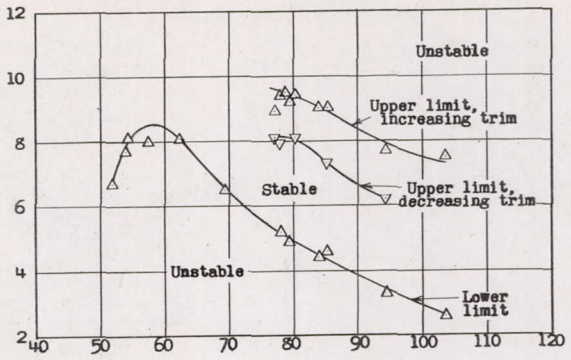

(a) $\beta = 20^{\circ}$.

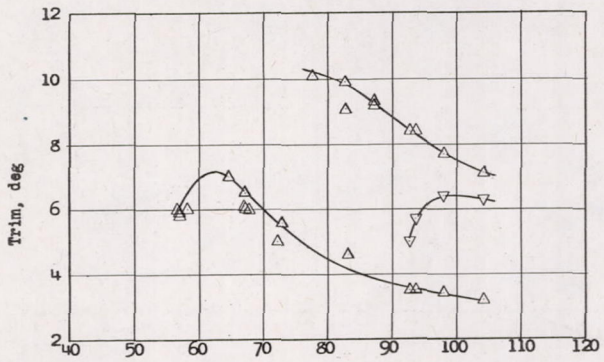

(b) $\beta = 40^{\circ}$.

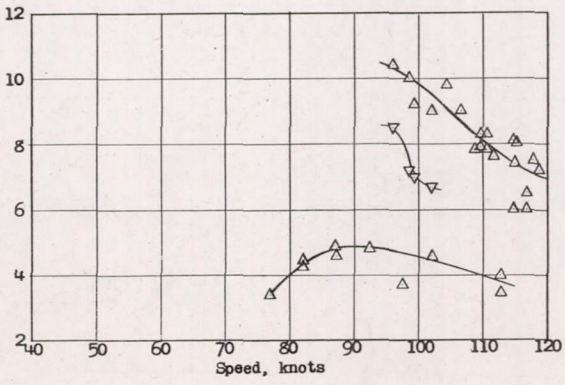

(c) $\beta = 60^{\circ}$.

Figure 4.- Trim limits of stability.

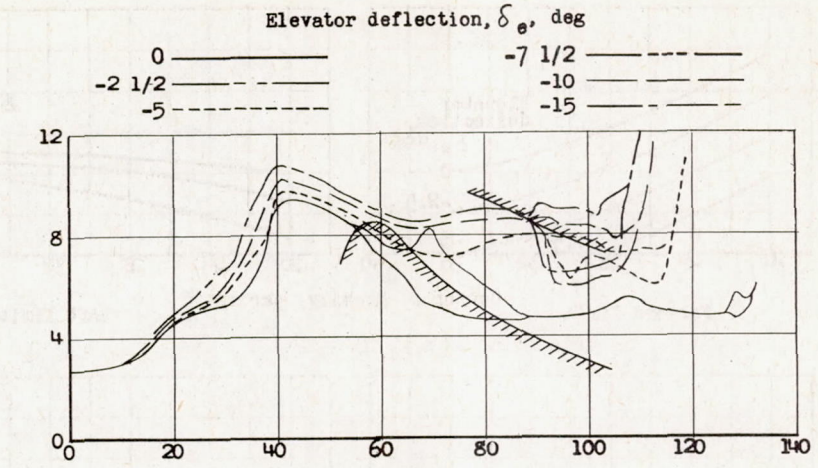

(a) $\beta = 20^\circ$.

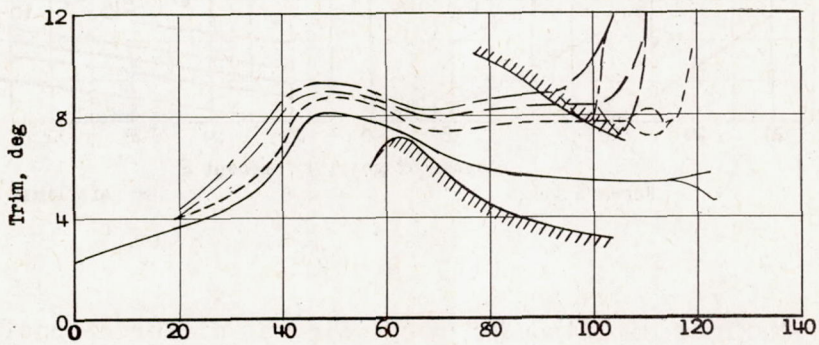

(b) $\beta = 40^\circ$.

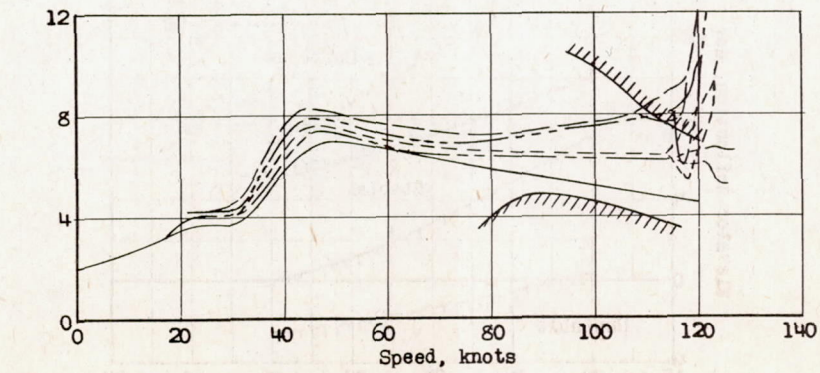

(c) $\beta = 60^\circ$.

Figure 5.- Variation of trim with speed, center of gravity at 28 percent $\bar{c}$. Trim limits are superposed.

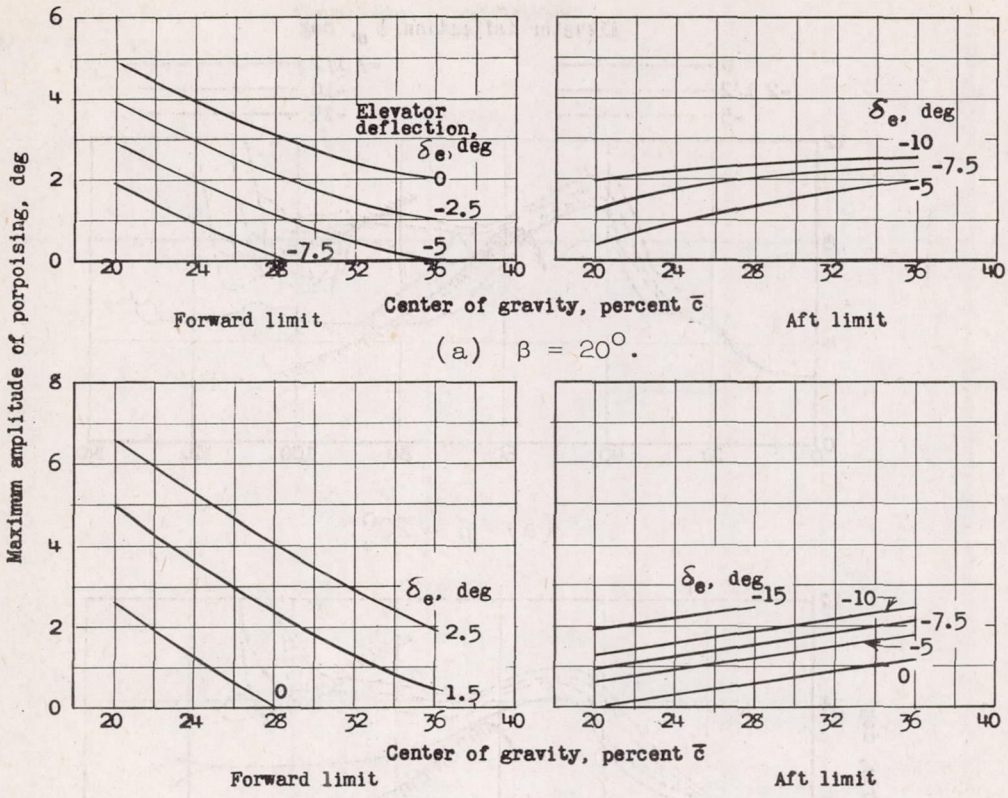

(a) $\beta = 20^\circ$.

(b) $\beta = 40^\circ$.

Figure 6.- Maximum amplitude of porpoising at different positions of the center of gravity. $\beta = 20^\circ, 40^\circ$.

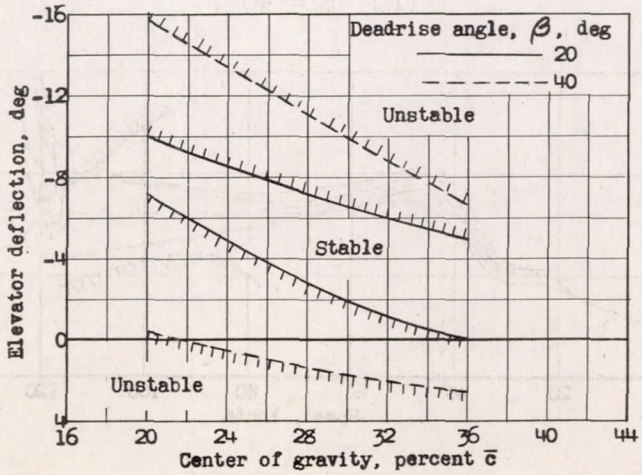

Figure 7.- Center-of-gravity limits of stability for 2° amplitude of porpoising. $\beta = 20^\circ, 40^\circ$.

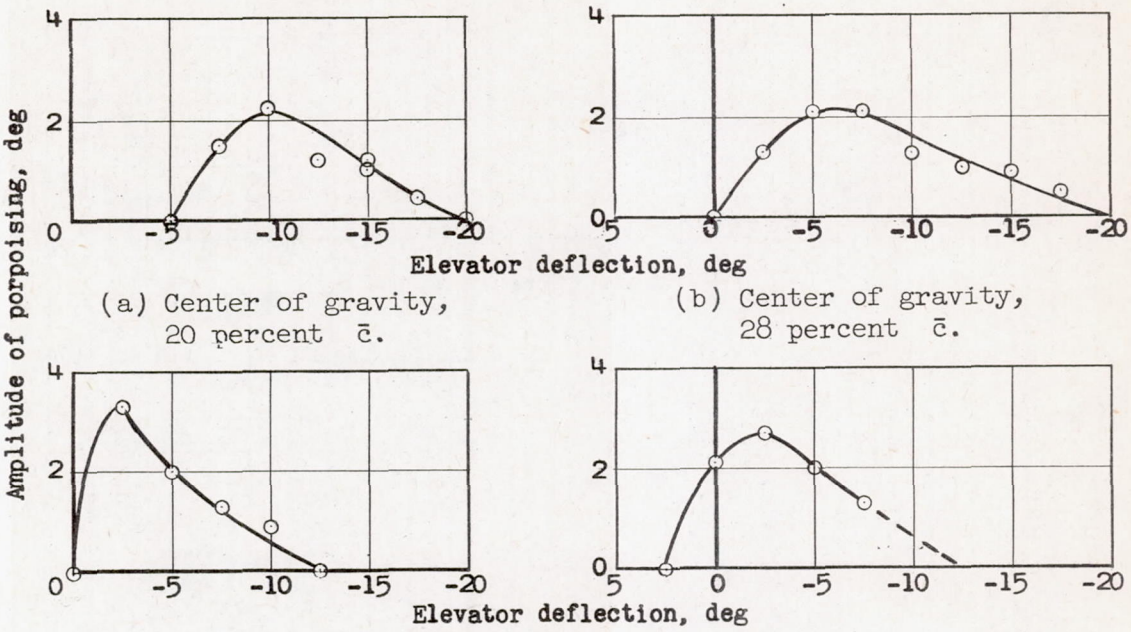

(a) Center of gravity, 20 percent $\bar{c}$.

(b) Center of gravity, 28 percent $\bar{c}$.

(c) Center of gravity, 36 percent $\bar{c}$.

(d) Center of gravity, 40 percent $\bar{c}$.

Figure 8.- Variation of maximum amplitude of upper-limit porpoising with elevator deflection at various center-of-gravity positions; $\beta = 60^{\circ}$.

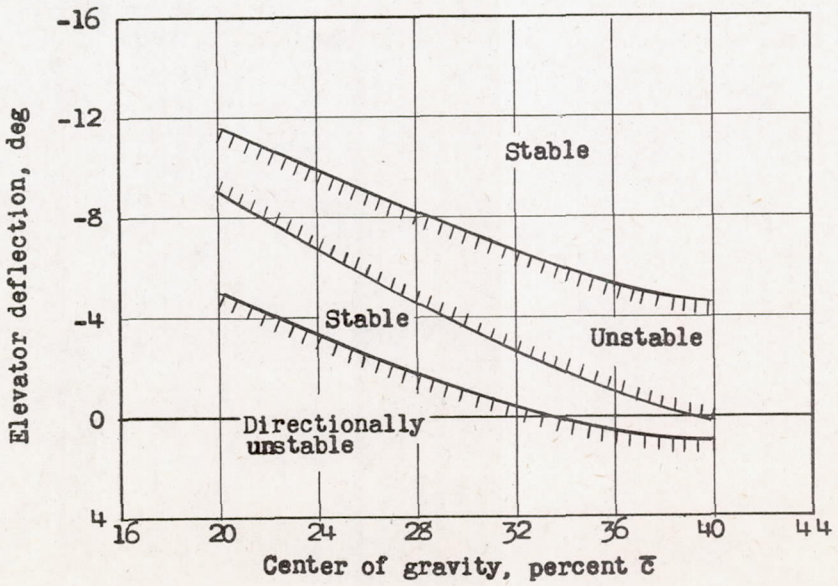

Figure 9.- Center-of-gravity limits of stability for 2° amplitude of upper limit porpoising together with minimum elevator deflections for directionally stable take-offs; $\beta = 60^{\circ}$.

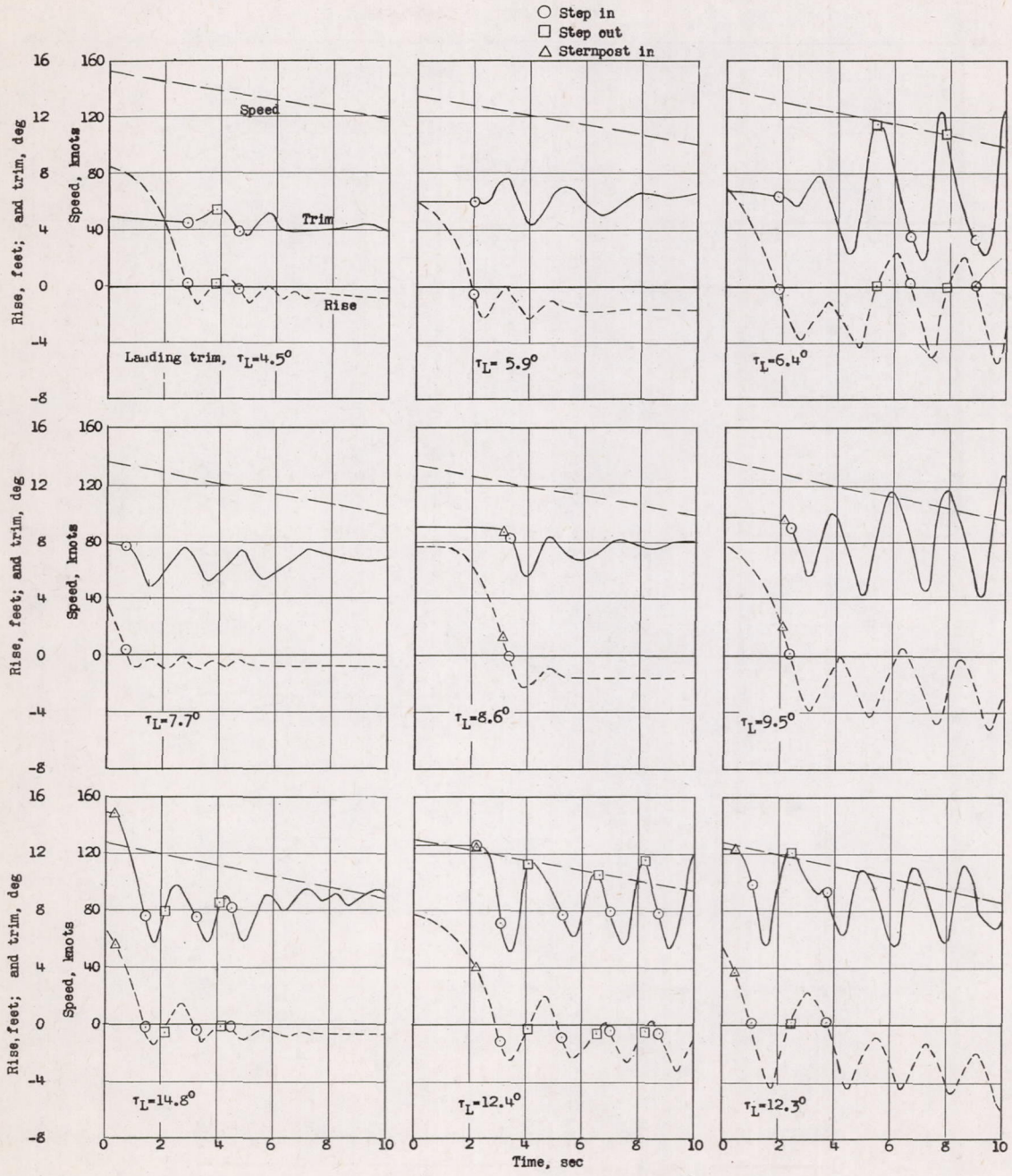

(a) $\beta = 20°$. (b) $\beta = 40°$. (c) $\beta = 60°$.

Figure 10.- Typical smooth-water-landing time histories.

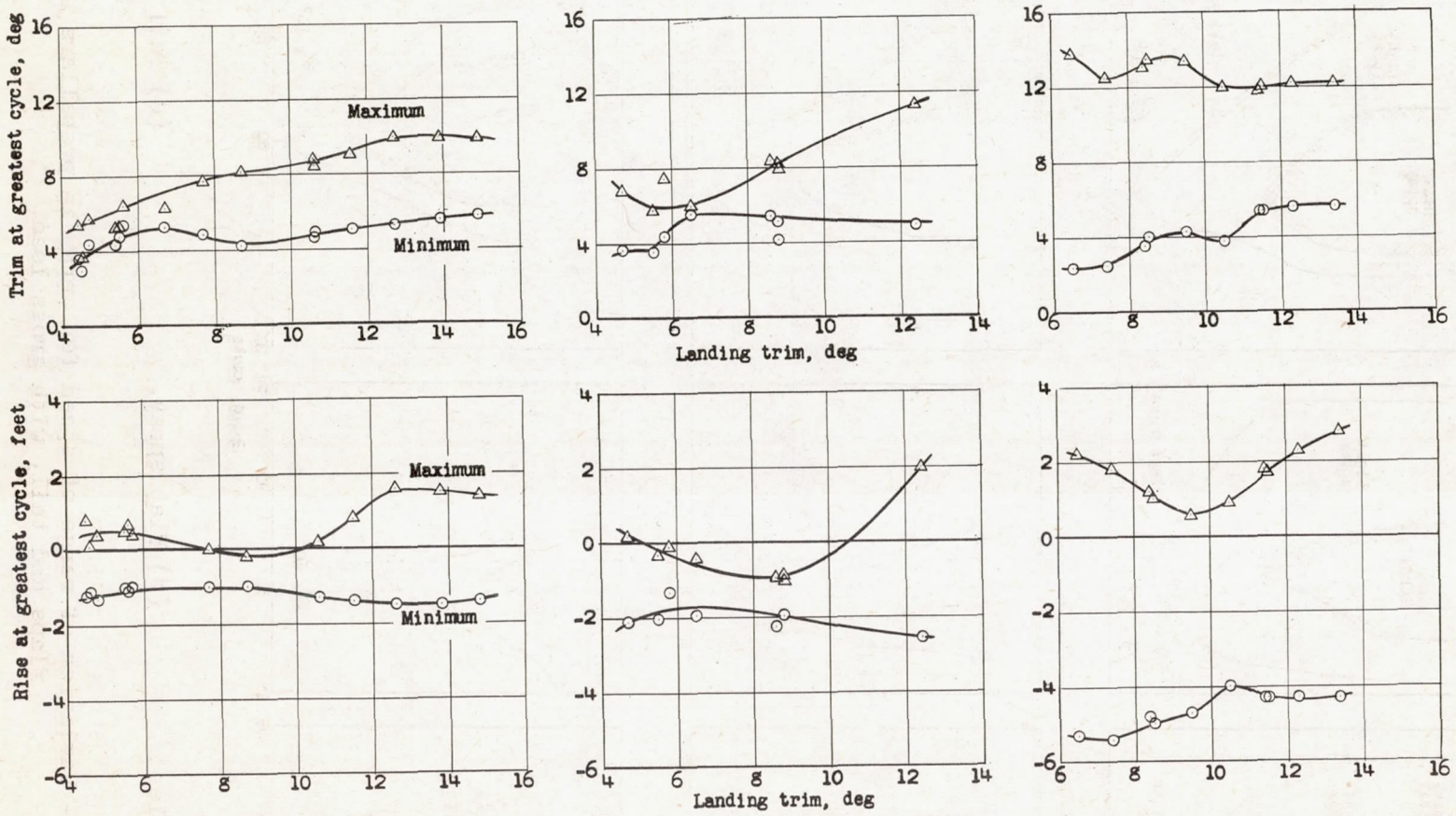

(a) $\beta = 20^{\circ}$. (b) $\beta = 40^{\circ}$. (c) $\beta = 60^{\circ}$.

Figure 11.- Variation of maximum and minimum trim and rise with trim at contact.

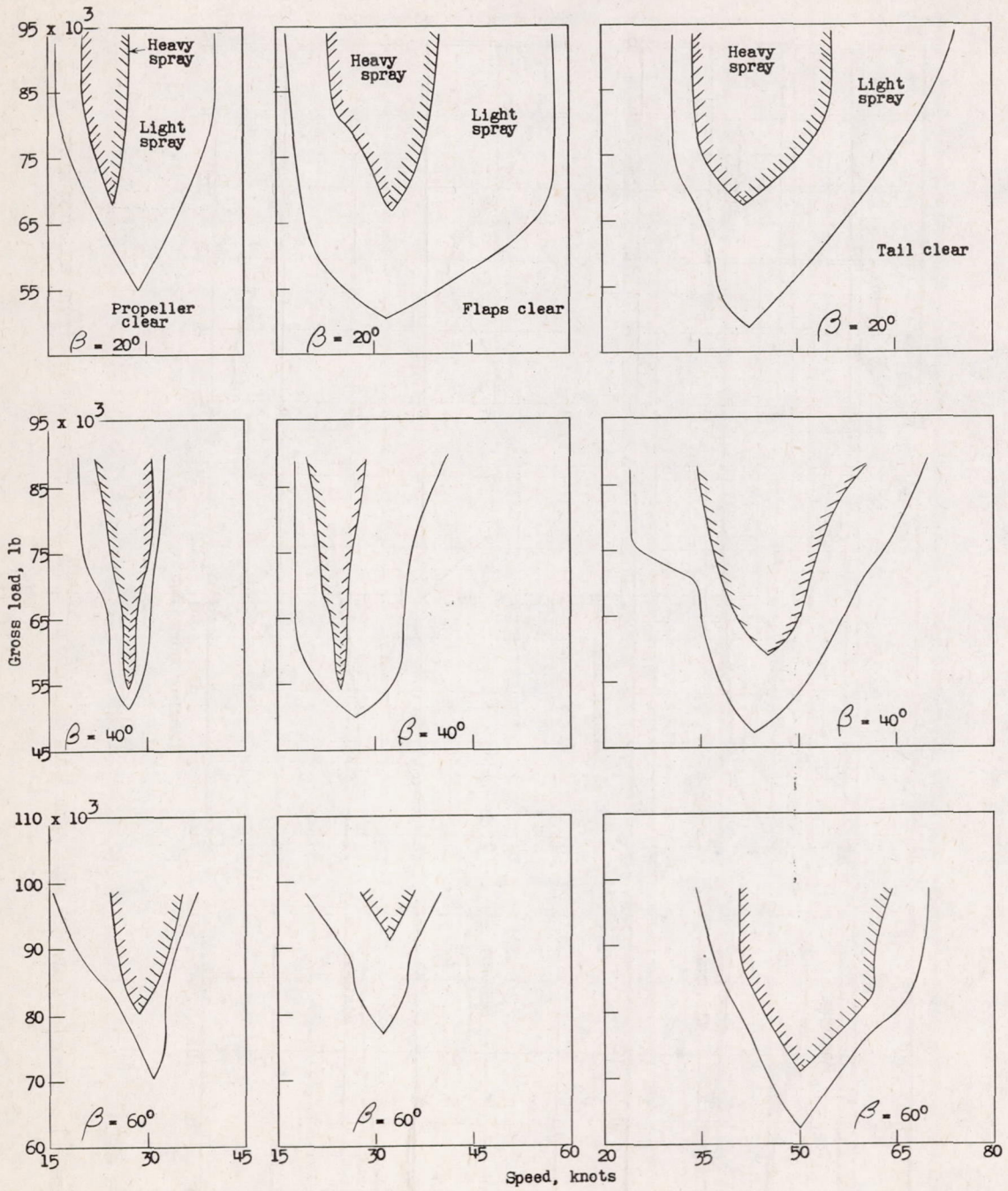

(a) Propeller spray.

(b) Flap spray.

(c) Tail spray.

Figure 12.- Variation of range of speed for spray in propellers and on flaps and tail, with gross load.

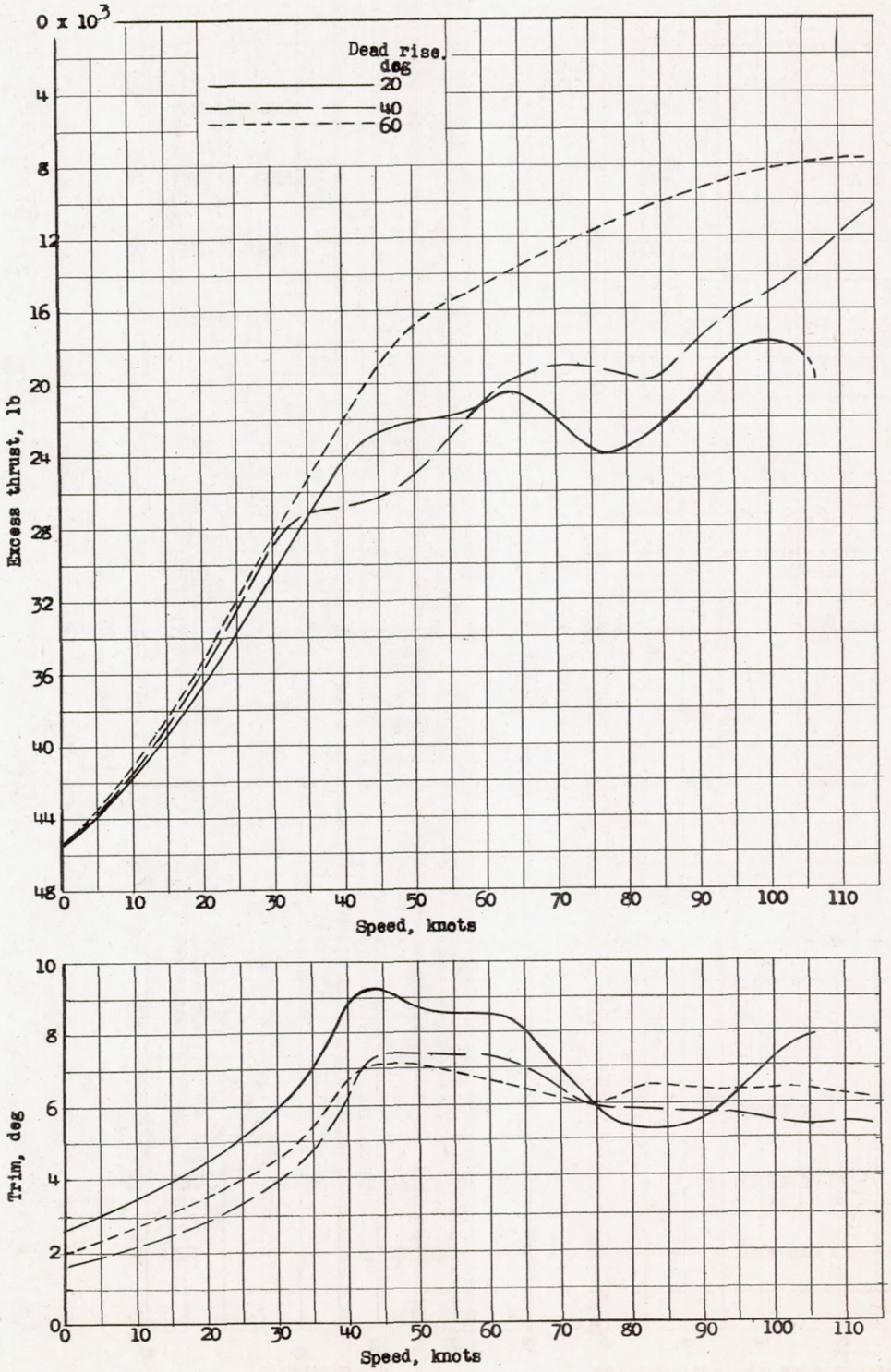

Figure 13.- Variation of excess thrust and trim with speed during take-off.

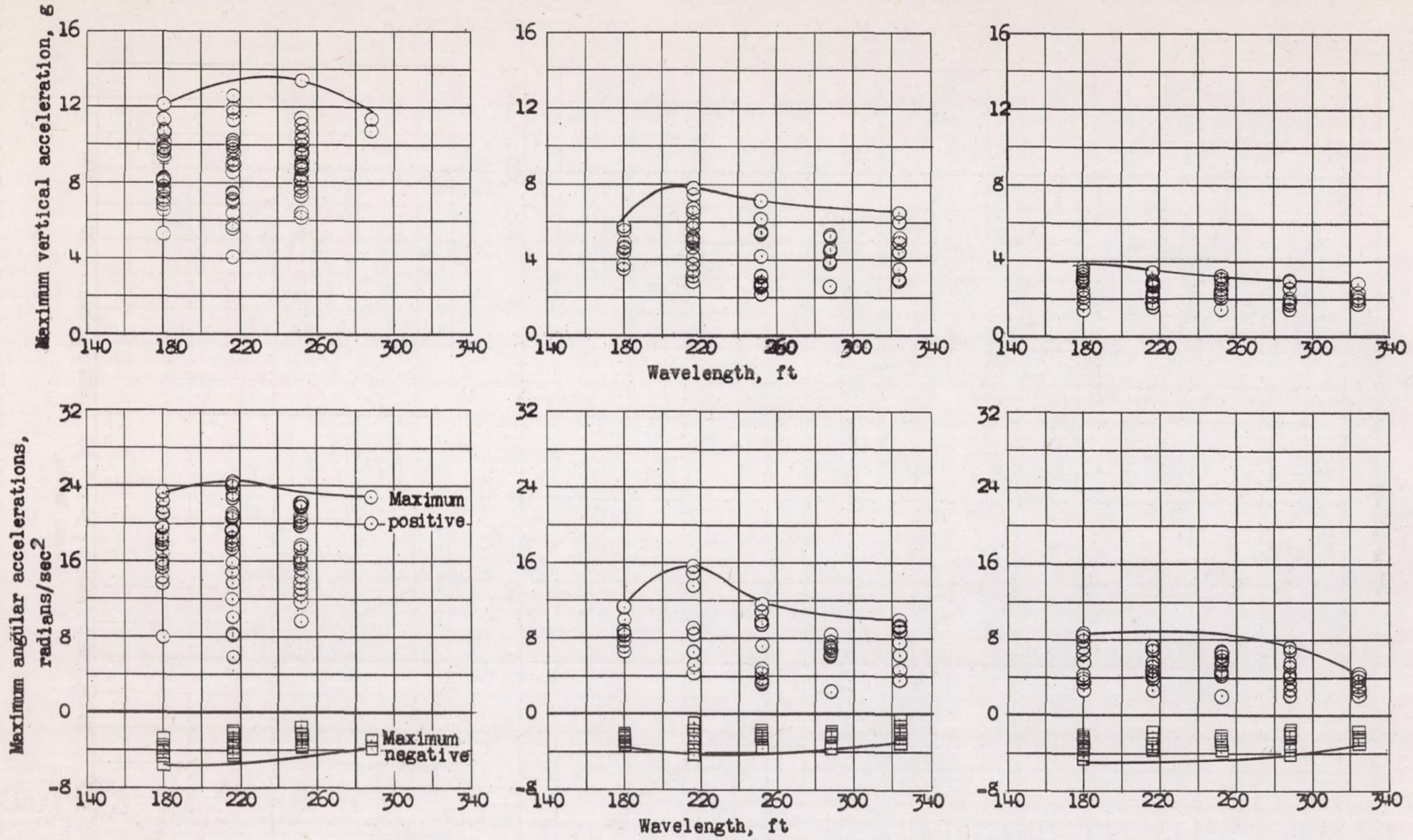

(a) $\beta = 20^\circ$. (b) $\beta = 40^\circ$. (c) $\beta = 60^\circ$.

Figure 14.- Variation of maximum vertical and maximum positive and negative angular acceleration with wavelength, for landings in waves 4 feet high.

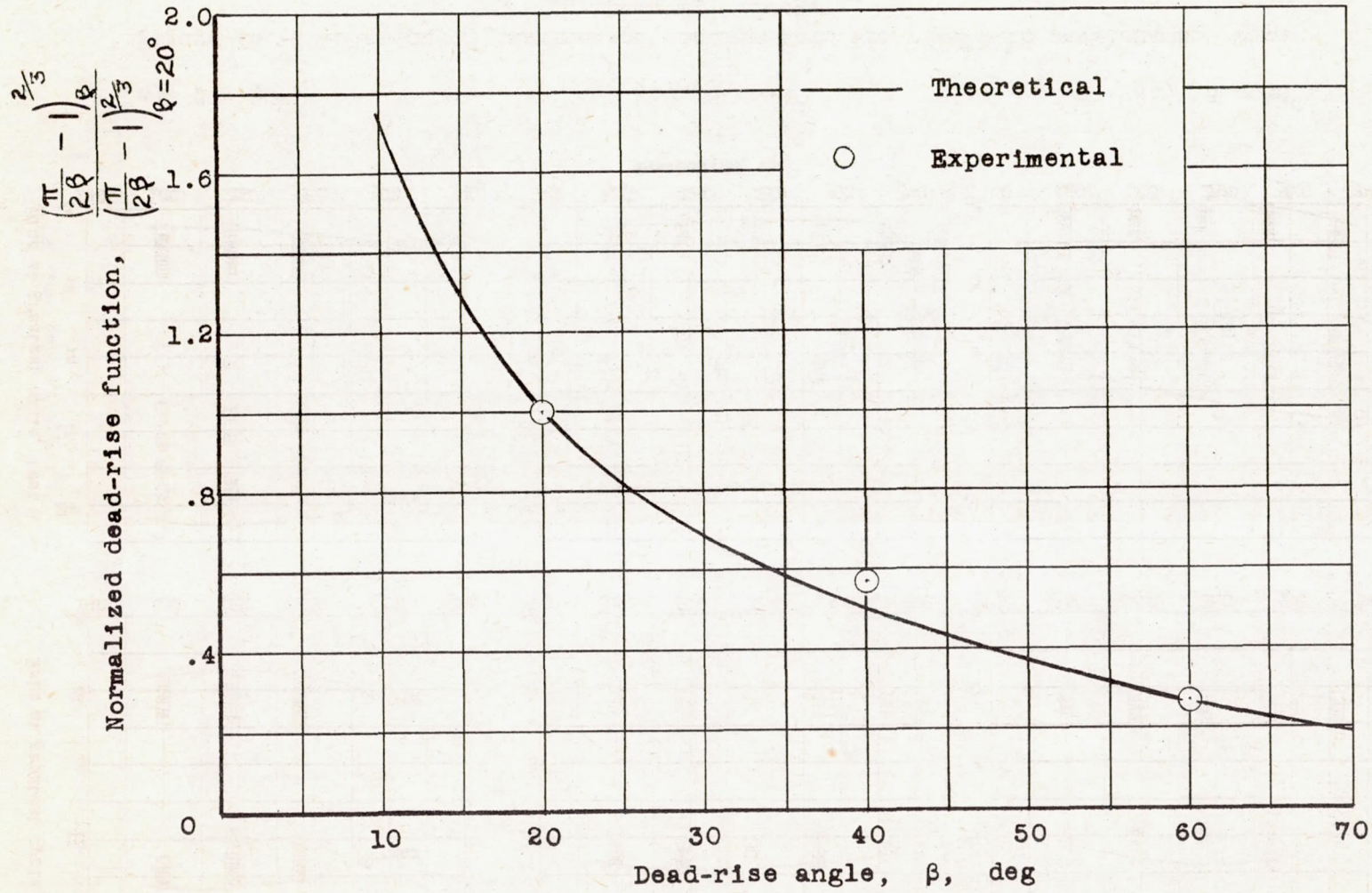

Figure 15.- Theoretical and experimental values of normalized dead-rise function.

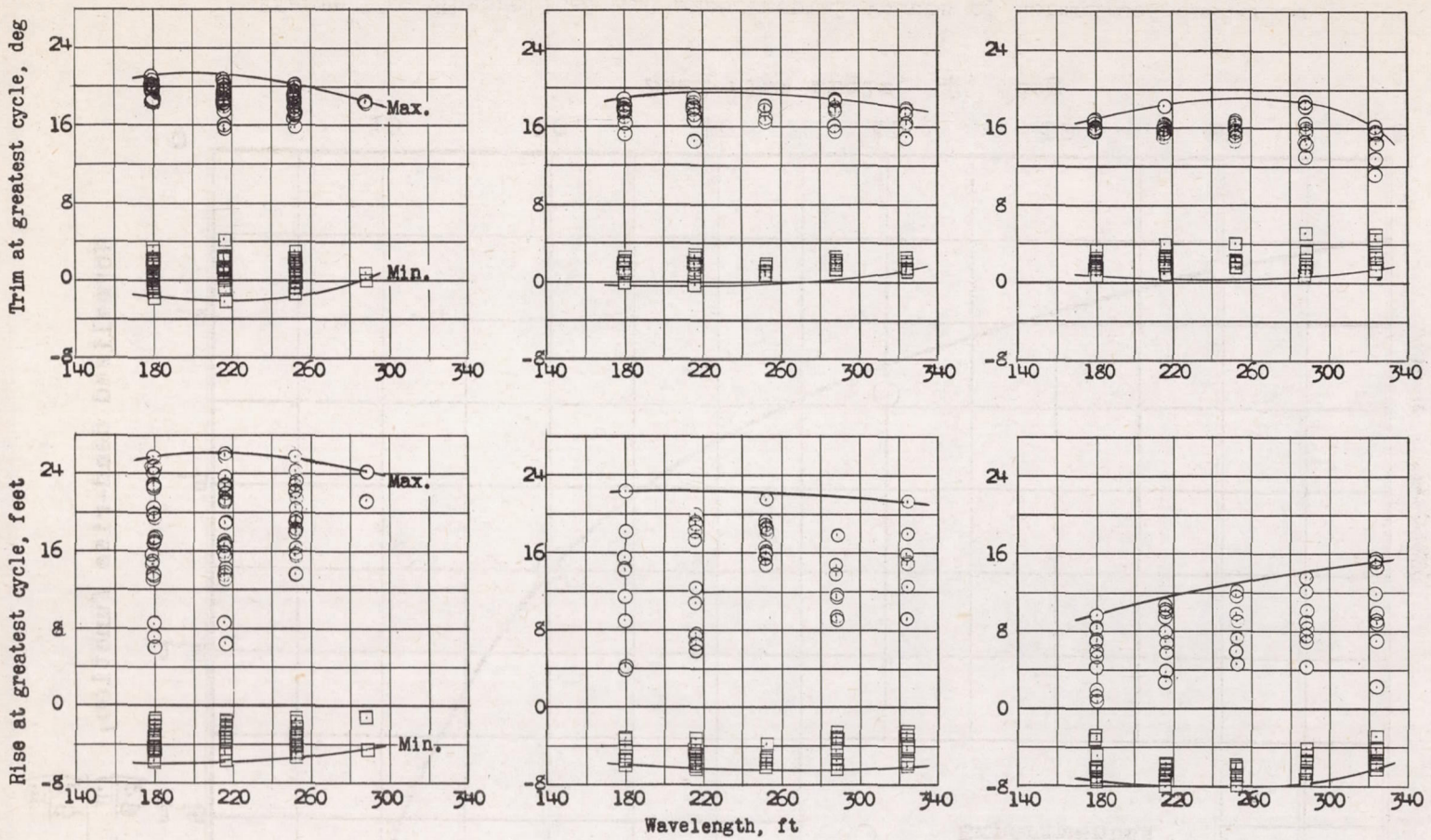

(a) $\beta = 20^\circ$. (b) $\beta = 40^\circ$. (c) $\beta = 60^\circ$.

Figure 16.- Variation of maximum and minimum trim and rise with wavelength. Wave height, 4 feet.